Modeling Intra- and Extra-Particle Processes of Wood Fast Pyrolysis

Colomba Di Blasi
Dipartimento di Ingegneria Chimica, Universitá degli Studi di Napoli "Federico II," 80125 Napoli, Italy

A detailed single-particle model, including a description of transport phenomena and a global reaction mechanism, is coupled with a plug-flow assumption for extraparticle processes of tar cracking, in order to predict the fast pyrolysis of wood in fluid-bed reactors for liquid-fuel production. Good agreement is obtained between predictions and measurements of product yields (liquids, char, and gases) as functions of temperature. Particle dynamics are very affected by the convective transport of volatile products. The average heating rates are on the order of 450–455 K/s, whereas reaction temperatures vary between 770 and 640 K (particle sizes of 0.1–6 mm and a reactor temperature of 800 K). The effects of several factors, such as size, shape, and shrinkage of wood particles, and external heat-transfer conditions are also examined.

Introduction

The development of alternative sources of energy and chemicals through biomass fuels is gaining continuous interest. Pyrolytic degradation, which in the early 1980s was hampered by a lack of specificity (Shafizadeh et al., 1979), is currently recognized as an effective route for the production of high yields of char (Antal et al., 1996, 2001) or liquid/gaseous fuels (Scott et al., 1999; Bridgwater, 1999). Commercial applications depend on the development of specific pyrolysis units and the understanding of the interaction between transport phenomena and reaction mechanisms, so that these can be better controlled or catalyzed to optimize the process. Mathematical modeling can be a useful tool for such purposes.

Reviews on the modeling of biomass pyrolysis (Di Blasi, 1993, 2000a; Gronli, 1996) reveal that comprehensive descriptions of single-particle processes are available. Analyses are mainly concerned with thick particles and/or slow external heat-transfer rates (conventional pyrolysis), whereas fast pyrolysis has been considered only in a few cases. These are focused on the behavior of isolated particles of cellulose undergoing radiative (Kothari and Antal, 1985; Di Blasi, 1996a) or contact (Di Blasi, 1996b) heating, and on both particle and extraparticle processes for fluid-bed conditions (Di Blasi, 2000b). The selection of cellulose comes from the inability of the majority of wood pyrolysis mechanisms to predict the correct dependence of product yields on temperature (Di Blasi, 1996c, 1998a), in some cases, even from the qualitative point of view. Although these studies have contributed to the understanding of pyrolysis fundamentals, cellulose is a fuel of little importance from the practical point of view, and the differences in the physical and chemical properties do not allow the results obtained for this fuel to be extended to wood/biomass. Hence further analysis is required as a basis for technological improvement of fast pyrolysis units, in particular, fluid-bed reactors.

The attainment of fast pyrolysis conditions in fluid-bed reactors is dependent on the characteristics of both the wood particles and the bed. Particle sizes for fast pyrolysis aimed at liquid-fuel production are reported to be in the range 0.1–6 mm (Bridgwater, 1999; Scott et al., 1999) with reactor temperatures roughly between 700 and 800 K. The gas-to-biomass feed rates depend upon the design of the conversion unit. With reference to the process based on a shallow fluid bed and indicated as Waterloo Fast Pyrolysis Process (WFPP) (Scott et al., 1999) they weigh between 6 and 9 (kg/kg), resulting in apparent volatile residence times, tv, of 0.3–0.8 s (defined as the net empty reactor volume divided by the inlet gas volumetric rate at reactor conditions). Also, recent findings (Scott et al., 1999) indicate that liquid yield and composition remain about the same as in the WFPP, if operating with a deep fluid-bed reactor (RTI process) with longer residence times, that is, 2–5 s, and again moderate temperatures.

Among the mechanisms of primary pyrolysis of wood, two exceptions in relation to predictions of product yields, at least for kinetic control, are those proposed by Wagenaar et al. (1994) for pine wood and, more recently, by Di Blasi and Branca (2001) for beech wood. Both kinetics are based on the

analysis of isothermal thermogravimetric data and product yields from laboratory-scale reactors by means of the one-stage mechanism originally introduced by Shafizadeh and Chin (1977). Neither of these two kinetic mechanisms has yet been applied to predict the characteristics of fast pyrolysis of wood, apart from engineering evaluations for the design and development of a rotating cone reactor (Wagenaar, 1994; Janse, 1998).

In this study, the reaction mechanism presented in Di Blasi and Branca (2001) is coupled with a model of intraparticle transport phenomena and extraparticle tar cracking (Di Blasi, 2000b) to simulate fast pyrolysis of wood in fluid-bed reactors, and to compare predictions and measurements of product yields. This study also provides particle heating rates, reaction temperatures and conversion times, and discusses the effects of some factors not addressed in previous literature, such as size, shape, and shrinkage of the wood particles and external heat-transfer conditions.

Mathematical Modeling

The pyrolysis dynamics of single particles are modeled so we can understand the role played by intraparticle processes on product distribution and determine the conversion time for particle sizes and heating conditions typical of fast pyrolysis. Extraparticle processes are also described, though in a simplified way. The model equations have already been presented elsewhere. In particular, those for slab-shaped, shrinking particles are reported by Di Blasi (1996c). The formulation for constant-volume cylindrical or spherical particles is reported in (Di Blasi, 2000b), where a detailed description of the models for the external heat-transfer coefficient and the extraparticle degradation of tars is also presented (for fluid-bed conditions). Only the chief characteristics of the reaction kinetics and the mathematical model are discussed here.

Reaction mechanism

The reactions of wood pyrolysis (Di Blasi, 2000a) can be roughly identified as primary solid degradation, which gives rise to products lumped into condensable (tars and water, usually labeled ''liquids'') and noncondensable (gases) volatiles and solid char, and secondary reactions of volatile condensable products to low-molecular weight gases and refractory tar (or char), which occur inside the reacting solid or the heating environment. Because wood is a heterogenous material, mainly consisting of cellulose, hemicellulose, and lignin, and minor amounts of extractives (a mixture of organic compounds that can be removed by solvents) and inorganics (ash), the thermogravimetric curves show the existence of several zones associated with the devolatilization of the different components (Antal and Varhegyi, 1995). Following this experimental observation, multistage reaction schemes of primary wood degradation have been proposed to describe the evolution of the main components or reaction zones (for example, Antal and Varhegyi, 1995; Gronli, 1996). Owing to the assumption of a constant ratio between the yields of char and volatiles, when coupled with the description of transport phenomena, these authors do not predict the variations in the yields of products with the operating conditions.

Reaction mechanisms describing the kinetics of product formation require the knowledge of the corresponding yields for each reaction stage. Given that accurate measurements of the volatile fractions cannot be accomplished for the small sample quantity used in thermogravimetric analysis and that laboratory-scale reactors only allow the total final yields to be obtained, no alternative is currently proposable to a one-stage mechanism of primary wood degradation. Hence, the mechanism with three parallel reactions for the formation of primary pyrolysis products, as originally proposed by Shafizadeh and Chin (1977) and used by other researches (for a review, see Di Blasi, 1998a; Di Blasi and Branca, 2001), is chosen here:

$$W \begin{cases} \overset{k_C}{\nearrow} \text{CHAR} \\ \overset{k_L}{\rightarrow} \text{LIQUIDS}, \\ \overset{k_G}{\searrow} \text{GAS} \end{cases} \qquad k = k_G + k_L + k_C, \qquad k_j = A_j e^{-E_j/(RT)}, \quad j = G, L, C \qquad (a1\text{–}a3; 1, 2).$$

Kinetic constants are those reported by Di Blasi and Branca (2001) ($E_G = 152.7$ kJ/mol, $A_G = 4.4 \times 10^9 \text{s}^{-1}$; $E_L = 148.0$ kJ/mol, $A_L = 1.1 \times 10^{10}$ s^{-1}; $E_C = 111.7$ kJ/mol, $A_C = 3.2 \times 10^9$ s^{-1}). The separate formation of the three product classes described by the reaction a1–a3 may be questionable (Antal, 1982, 1985a) from the point of view of analytical chemistry. However, as already shown for cellulose (Di Blasi, 1993), their comparable activation energies do not allow the selectivity to be displaced toward only one of the products. Also, for kinetic control, they correctly predict the continuous increase of both liquid and gas products at the expense of char as the reaction temperature is increased (Di Blasi and Branca, 2001). Given that holocellulose is converted mainly into liquids, the other two product classes (gases and char) are essentially due to lignin degradation. Hence, at low temperatures, on a global basis, there is a competition between liquid (holocellulose degradation) and char (lignin degradation) formation, with the former becoming successively more favored. At high temperatures, gas formation rates tend to increase, owing to the faster devolatilization rates of lignin.

Kinetic constants for the reactions a1–a3 (Di Blasi and Branca, 2001) were obtained by minimizing the activity of secondary reactions. Indeed, isothermal (temperature range 573–708 K) weight-loss curves of thin layers of beech wood powder were measured under a forced nitrogen flow, which created the inert environment, reduced the residence time of vapors inside the reaction chamber, and cooled both the gas-phase environment during pyrolysis and the solid residue after complete devolatilization. The size of the wood layer was determined so that, for the most severe thermal conditions (heating rate of 1,000 K/s and a final temperature of 708 K), the char yield remained constant, an indication of negligible temperature gradients (primary char) and residence times of primary volatile products (secondary char) across the sample. The yields of volatile products to be associated with the weight-loss curves were also determined for negligible activity of secondary reactions. Indeed, for low temperatures (< 650 K), when secondary reactions are barely active, mea-

surements were carried out for solid residence times sufficiently long for complete conversion. For higher values (range 650–708 K), the data provided by Scott and Piskorz (1984) and Scott et al. (1988), where the very small volatile residence times again hindered significant degradation of tars, were used.

The most general global mechanism for secondary reactions of primary tars was proposed by Antal (1983, 1985b)

$$\text{LIQUIDS} \begin{cases} \xrightarrow{k_{S1}} \text{GAS} \\ \xrightarrow{k_{S2}} \text{REFRACTORY TARS} + \text{H}_2\text{O} \end{cases} \qquad \text{(a4–a5)}$$

$$k_S = k_{S1} + k_{S2}, \qquad k_j = A_j e^{-E_j/(RT)}, \qquad j = S1,\ S2 \qquad (3, 4)$$

The mechanism involves the gas-phase cracking of volatiles to permanent gas species (k_{S1}) and the gas-phase polymerization of volatiles to a refractory condensable (tar/char) product and some water (k_{S2}). However, apart from the estimation of the kinetic constants for cellulose tars and the differences between the activation energies of the two reactions for lignin tars (Antal, 1983, 1985b), both kinetic and transport models always considered only the cracking reaction a4 (Di Blasi, 2000a). The same treatment is also retained here for the intraparticle processes with reaction kinetics derived from Liden et al. (1988). For extraparticle processes, different kinetic parameters for the reaction a4 derived for wood tars and both the reactions a4–a5 are compared, with the kinetic parameters provided by Antal (1983) for cellulose tars.

Finally, as already assumed for cellulose (Di Blasi, 2000b), primary char and gas formation and tar cracking are exothermic processes, whereas tar formation/vaporization is an endothermic process.

Transport phenomena

In the description of intraparticle transport phenomena the following assumptions are made: (1) local thermal equilibrium, (2) perfect gases, (3) negligible kinetic and potential energy and replacement of internal energy with enthalpy, (4) negligible enthalpy flux due to species diffusion and body forces, (5) no moisture content. The main physical processes taken into account include: (1) property variation with the conversion level, (2) accumulation of volatile species mass and enthalpy within the pores, (3) heat transfer by convection, conduction, and radiation, (4) convective and diffusive transport of volatile species, (5) gas pressure and velocity variations (Darcy law), and (6) volume variation. For point (6), a simplified version of the model proposed in (Di Blasi, 1996c) is applied, because in fast pyrolysis the large amount of volatiles released is certainly the main factor responsible for variations in the particle volume. Indeed, it is assumed that the total volume may decrease in proportion to the mass of volatiles generated from the degradation process.

The particle, at ambient temperature, is suddenly exposed in a hot (T_r) inert medium (reactor). Given the symmetry of the problem, only half a particle is simulated. Therefore, while the particle center ($x = 0$) is subjected to conditions of zero gradients on the variables, the external surface ($x = \tau$) is exposed to heating. The external heat-transfer coefficient at the particle surface is representative of conditions established in fluid-bed reactors. This transfer is made by two contributions, the first corresponding to overall convective transport and the second to radiation. The first contribution makes use of the model proposed by Agarwal (1991), as already discussed in (Di Blasi, 2000b). The effect of the efflux of volatiles generated as a consequence of the degradation process on the heat transfer to the particle is taken into account through the introduction of a correction factor (Stewart, 1984).

The description of extraparticle processes is highly simplified. All the particles experience the same thermal (and conversion) history. In addition, the organic fraction (tars) of liquids (tars and water) produced undergo extraparticle cracking according to an apparent residence time, t_v, defined as in Scott et al. (Scott and Piskorz, 1984; Scott et al., 1988), or to a residence time, t_b, evaluated as in Di Blasi (2000b), that is, with reference to the expanded bed height and the bubble velocity. Reactions occur at the reactor temperature (T_r).

Table 1. Particle Properties and Reactor Characteristics

	Particle	*Reactor*
$B_S = 5\times10^{-16}$ m^2	Estimated	$D_r = 0.1$ m
$B_C = 1\times10^{-13}$ m^2	Estimated	$d_s = 150$ μm
$c_S = 1.4$ kJ/kg·K	Di Blasi (2000b)	$H = 0.106$ m
$c_L = 1.2$ kJ/kg·K	Gronli (1996)	$L = 0.50$ m
$c_g = 1.1$ kJ/kg·K	Gronli (1996)	$U_{mf} = 0.0108$ m
$c_C = 1.1$ kJ/kg·K	Di Blasi (2000b)	$W = 1$ kg
$D_0 = 0.2\times10^{-4}$ m^2/s	Di Blasi (2000b)	
$d_S = 4\times10^{-5}$ m	Di Blasi (2000b)	
$d_C = 4\times10^{-4}$ m	Di Blasi (2000b)	
$e_S = 0.92$	Gronli (1996)	
$e_C = 0.7$	Gronli (1996)	
$\epsilon = 0.4$	Gronli (1996)	
$\lambda_S = 2.09\times10^{-1}$ W/m·K	Gronli (1996)	
$\lambda_C = 7.1\times10^{-2}$ W/m·K	Gronli (1996)	
$\lambda_g = 25.77\times10^{-3}$ W/m·K	Di Blasi (2000b)	
$\mu = 3\times10^{-5}$ kg/m·s	Di Blasi (2000b)	
$\rho_{S0} = 700$ kg/m^3	Gronli (1996)	
$\omega = 1$	Di Blasi (2000b)	

Results

Particle properties are roughly those of beech wood for perpendicular grain heating with properties of volatiles reproducing, on the average, the values reported in the literature (Table 1). In order to define external heat-transfer coefficients and extraparticle volatile residence times, a pilot-scale fluid-bed reactor (Scott and Piskorz, 1984; Scott et al., 1988) is chosen with a superficial velocity assigned as $U_0 = 10\times U_{mf}$, resulting in $t_b = 0.154$ s (Di Blasi, 2000b).

A first set of simulations has been made with nonshrinking, slab-shaped particles in the absence of extraparticle processes to simulate the effects of reactor temperature, particle size, and external heat-transfer coefficient. A parametric investigation has also been carried out about the influences of particle shrinkage and shape.

A second set of simulations has been made by coupling the models of single-particle and extraparticle processes. The effects of the volatile residence time and secondary degrada-

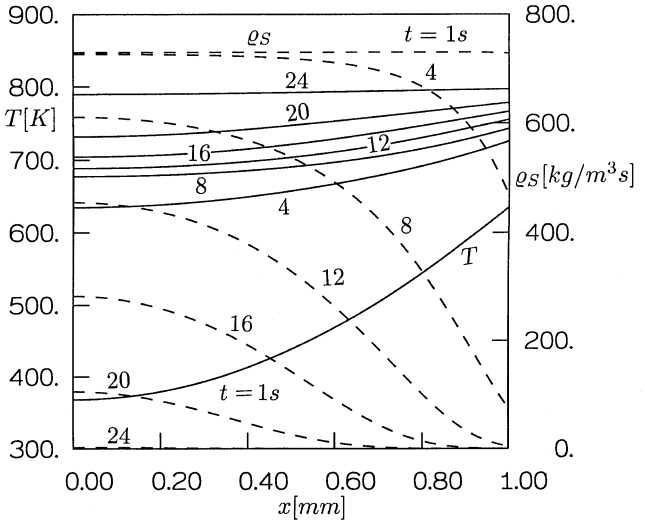

Figure 1. Spatial profiles of temperature (—) and wood density (– – – –).

$\tau = 1$ mm and $T_r = 800$ K for $t = 1$, 4, 8, 12, 16, 20, 24 s (single-particle model).

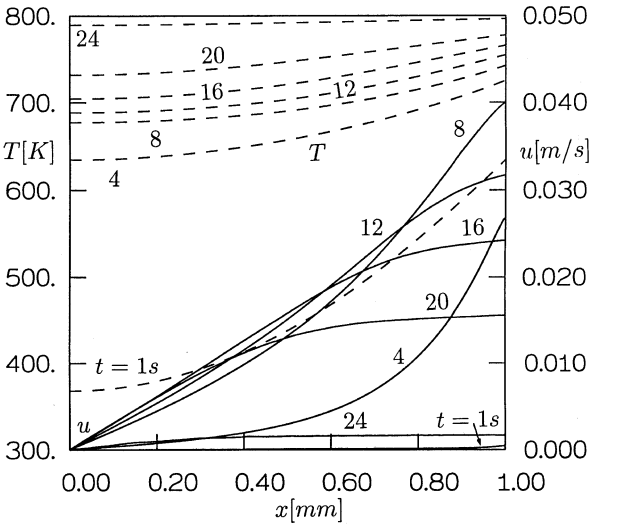

Figure 2. Spatial profiles of temperature (– – – –) and gas velocity (—).

$\tau = 1$ mm and $T_r = 800$ K for $t = 1$, 4, 8, 12, 16, 20, 24 s (single-particle model).

tion kinetics of tars on the yields of liquids and gas have been simulated. Finally, in order to assess the validity of model predictions from the quantitative point of view, the experimental results reported by Scott and Piskorz (1982,1984), Scott et al. (1988), and Wehlte et al. (1997) have been simulated.

Influences of particle size and external temperature

Simulations for slab-shaped particles have been made by varying the half-thickness between 0.1 and 5 mm ($T_r = 800$ K) and the reactor temperature from 700 K to 1,100 K (particle half-thicknesses of 1 and 5 mm). External heat-transfer coefficients evaluated according to the model proposed by Agarwal (1991) are contained between 1,880 and 480 W/m^{2}K as τ varies in the range given earlier. Because the dependence of the external heat transfer on temperature is weak, simulations concerned with the effects of the reactor temperature used a heat-transfer coefficient evaluated at 800 K.

An example of particle dynamics is shown in Figures 1 and 2, in terms of spatial profiles of temperature, wood density, and gas velocity for $\tau = 1$ mm and $T_r = 800$ K. Temperature gradients are large only during the initial inert heating stage. Degradation is initially ($t \leq 2.5$ s) localized along a thin superficial layer, when the temperature attains values of about 600 K. Then the degradation front enlarges to the entire particle thickness and the spatial temperature gradients are highly reduced.

In accordance with previous analyses, reaction endothermicity (Narayan and Antal, 1996; Di Blasi, 1996a) and convective cooling, caused by the flow of volatiles products out from the particle (Di Blasi, 1998b; Stubington and Sasongko, 1998; Di Blasi, 2000b), introduce significant delay in particle heating, so that the temperature remains almost constant (below 700 K for wood and the conditions of Figures 1 and 2) as long as decomposition reactions are active. For this reason, wood pyrolysis has been sometimes referred to as a fusion-like (phase change) phenomenon (Narayan and Antal, 1996). A comparison of the magnitude of the contributions (reaction energetics, heat convection, and conduction) in the enthalpy equation was already provided by Di Blasi (1998b). It can be observed that convective transport is very important and, apart from the values of temperature and velocity (maximum of about 4×10^{-2} m/s with negligible overpressures for the case under study), it is directly proportional to the specific heats of volatile products. As the degradation process approaches completion, the particle heating rate restarts to increase.

The profiles of Figures 1 and 2 show that the heating rate and the reaction temperature established during wood degradation are affected by the conversion degree. In order to characterize the process in terms of global parameters, as in a previous study (Di Blasi, 2000b), the particle center temperature, T_c, and the heating rate, β, are examined, again with respect to the particle center. The variables T_c and β are reported in Figure 3 ($T_r = 800$ K) as functions of the particle half-thickness for low ($Y = 0.8$), intermediate ($Y = 0.5$), and high ($Y = 0.25$) conversion levels. As expected, the heating rate becomes successively slower as the particle size is increased, and/or successively higher conversion levels are considered because of enhanced internal heat-transfer resistance and convective cooling caused by volatile release. For the smallest particle size considered here ($\tau = 0.1$ mm), β varies from about 760 K/s ($Y = 0.8$) to 460 K/s ($Y = 0.5$) and 290 K/s ($Y = 0.25$). These figures are significantly lower for $\tau = 1$ mm and correspond to about 57, 34, and 23 K/s for the same conversions as before. For $\tau \geq 2$ mm, the maximum heating rates at the particle center are contained between 20 and 4.5 K/s, a clear indication of the importance of internal heat-transfer resistances. It is worth noting that these figures are much lower (in the best case, by one order of magnitude) than those reported for fluid-bed pyrolysis (Scott and Piskorz,

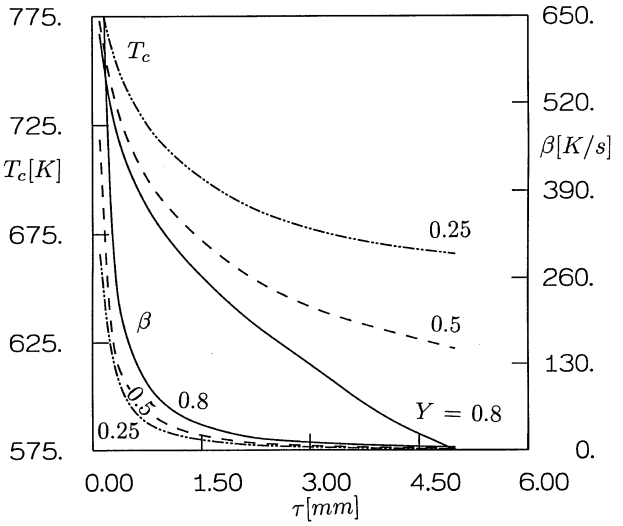

Figure 3. Temperature, T_c, and heating rate, β, at the particle center when the total mass fraction equals 0.8 (—), 0.5 (– – – –), and 0.25 (— · · — · ·) as functions of the half-thickness of the particle for $T_r = 800$ K (single-particle model).

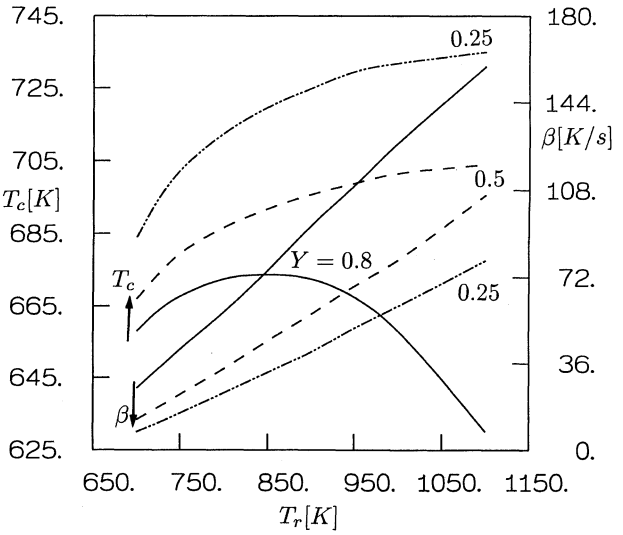

Figure 4. Temperature, T_c, and heating rate, β, at the particle center when the total mass fraction equals 0.8 (—), 0.5 (– – – –), 0.25 (— · · — · ·) as functions of the reactor temperature for $\tau = 1$ mm (single-particle model).

1984), usually estimated for μm-sized, inert particles in the absence of external heat-transfer resistance (an issue to be examined later).

As degradation takes place ($Y = 0.8 - 0.25$), the particle center temperature varies between 765 and 785 K ($\tau = 0.1$ mm), 670 and 710 K ($\tau = 1$ mm) and 575 and 665K ($\tau = 5$ mm). Hence, the fluid-bed conversion of wood particles for conditions typical of fast pyrolysis technologies ($\tau = 0.5-1.5$ mm), occurs with actual reaction temperatures significantly lower than those of the external environment and within the ranges examined in thermal analysis (Antal and Varhegyi, 1995; Gronli, 1996). The differences between T_c values at different conversion levels and between T_c and T_r decrease as successively thinner particles are pyrolyzed. However, in relation to the possibility of reaching high temperatures by very small-sized samples (a problem of interest in kinetic analysis carried out through fluid- and entrained-bed reactors), it should be observed that the reaction never occurs at the external (reactor) temperature and that the differences during the conversion are of about 40–90 K already for $\tau = 0.1-0.25$ mm.

For thick particles ($\tau \geq 3$ mm), as a consequence of internal heat-transfer control, the temperatures attained at the completion of the degradation process tend to become independent of the particle size (values of about 650 K). Also, for low conversions ($Y \leq 0.5$), the differences in T_c values are small, indicating that, once the degradation process begins, the convective cooling and reaction endothermicity keep the reaction temperature at an almost constant value. As a consequence of the small variation in the actual degradation temperature, it can be expected that the selectivity of primary reactions is scarcely affected by the particle size, though the successively thicker char zone may affect the secondary degradation of tar vapors.

The influences of the external temperature on the heating rate and reaction temperature can be seen in Figure 4 ($\tau = 1$ mm). Again, the heating rate decreases and the center temperature increases for successively higher conversions. Also, there is an almost linear increase in the particle heating rate with the external temperature. For instance, for low conversions ($Y = 0.8$), the temperature varies from about 25 K/s to to 150 K/s as T_r is varied from 700 K to 1,100 K ($Y = 0.8$). Although these values are noticeably lower when referred to high conversion levels (from 7 K/s to 75 K/s), fast pyrolysis can be accomplished either with small particles or high external temperatures, though because of secondary reaction activity, product distribution may be different.

The particle center temperature shows a relatively rapid increase with the external temperature only for values of this below 850 K, and then tends to become constant [for high conversions ($Y = 0.5-0.25$), maximum values of 703–735 K] or to decrease [for low conversions ($Y = 0.8$), maximum value 630 K). This is the consequence of both the successively more important role played by internal heat transfer (higher spatial temperature gradients) as the external temperature is increased, and the narrow temperature range where wood decomposition takes place. Therefore, the increase in the external temperature causes an increase in the heating rate but, unless the external temperatures are low so that chemical reaction rates are slow, the variations in the actual particle degradation temperature and selectivity of primary reactions are small. However, successively higher temperatures along the already charred region of the particle may again affect the activity of secondary reactions. Moreover, in relation to kinetic analysis, it can be expected that conversion temperatures much higher than those established in thermal analysis can be reached, when working with very small particles and external temperatures much higher than those used in fast pyrolysis, if the sample temperature is controlled effectively

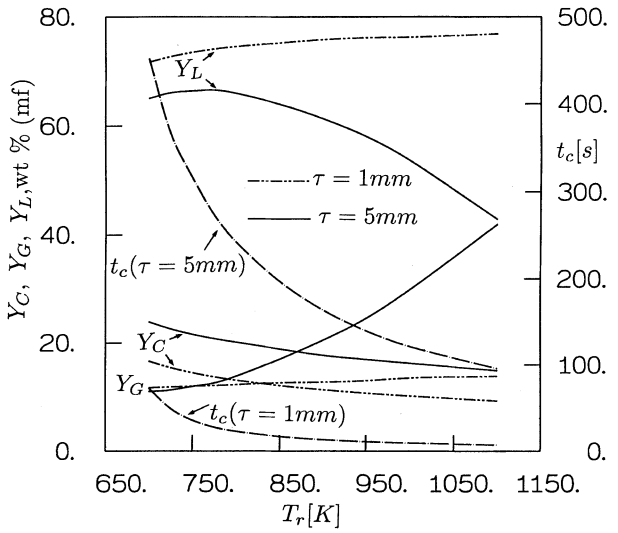

Figure 5. Product yields and conversion times as functions of the reactor temperature as predicted for $\tau = 1$ and 5 mm (single-particle model).

(Lanzetta et al., 1997). In this case, however, the activity of secondary reactions may become significant.

The dependence of the final product yields, expressed as percent of the initial wood weight (wt.) on a moisture-free (mf) basis, and the conversion time on the reactor temperature are shown in Figure 5 for two particle sizes ($\tau = 1$ and $\tau = 5$ mm). As expected, the char yields decrease as the external temperature is increased and/or the particle thickness is decreased, owing to the successively higher reaction temperatures established during primary degradation and the displacement of reaction selectivity toward volatile formation. In particular, for $T_r = 800$ K, the yields of char vary from about 8% to 17.5% for $\tau = 0.1$–3 mm. In accordance with the analysis presented earlier, the variations in the char yields are observed especially for T_r below 850 K.

For thin particles ($\tau = 1$ mm) both the liquid and the gas yields increase with temperature but, given the relatively low reaction temperatures (below 735 K, see Figure 4) and the slightly lower activation energy of liquid formation with respect to gas formation, the diminution in the char production appears mainly as a corresponding increase in the liquid yields (maximum of about 77%). Also, the continuous increase of the liquid yields with temperature indicates that intraparticle activity of secondary reactions is negligible for this particle size.

Significant degradation of tars (no distinction is made for intraparticle processes between the aqueous and organic fractions of liquids produced) to gas occurs mostly for thick particles ($\tau = 5$ mm) and external temperatures above 800 K. These findings are in qualitative agreement with experiments carried out for thick particles (Chan et al., 1985; Gronli, 1996; Di Blasi et al., 2000, 2001a,b).

As for the dependence of the conversion time on the particle size, it has been found to vary from 2.5 s to 241 s for $\tau = 0.1$–5 mm $T_r = 800$ K. Also, for $\tau = 1$ mm, conversion times becomes shorter than 60 s only for an external temperature above 750 K and, even for the highest temperature examined, they still remain about one order of magnitude longer than the residence time of volatile products (about 12 s against 0.5–1 s). In the other case ($\tau = 5$ mm), even for high temperatures (800–1,100 K), complete conversion requires several (4–1.5) minutes.

Given that for conditions of interest in fast pyrolysis intraparticle degradation of tars is small and that a competition exists mainly between char and liquid formation from primary degradation, in the following the analysis of single-particle processes will be made by means of char yields and conversion times.

Influences of the particle shrinkage and shape

Experiments (Gronli, 1996; Di Blasi et al., 2001b) show that thick particles undergo significant shrinkage (size reductions of 20–30%). This effect is important and should be taken into account by mathematical models (Di Blasi, 1996c) in order to get quantitative predictions of temperature profiles along the degrading particles. Particle shape can be another important factor for the pyrolysis characteristics, given that it affects the surface-to-volume (mass) ratio. Since a quantitative evaluation of the role played by these factors in fast pyrolysis is not available, simulations were carried out for slab-shaped particles for two values of the shrinkage factor— $\alpha = 0$ and 0.5 (reductions in the total particle volume by the entire and half-fraction of the volume initially occupied by volatile products, respectively)—and for nonshrinking spherical particles, by varying τ from 0.1 mm to 5 mm and $T_r = 800$ K.

Figures 6 and 7 report the char yields and the conversion times as functions of τ, as simulated for slabs with different shrinkage factors, and for nonshrinking spheres. Solutions obtained for nonshrinking slabs ($\alpha = 1$) are considered for comparison. The effects of both shrinkage and shape are significantly dependent on the particle size, but in all cases the char decreases and the conversion times become successively

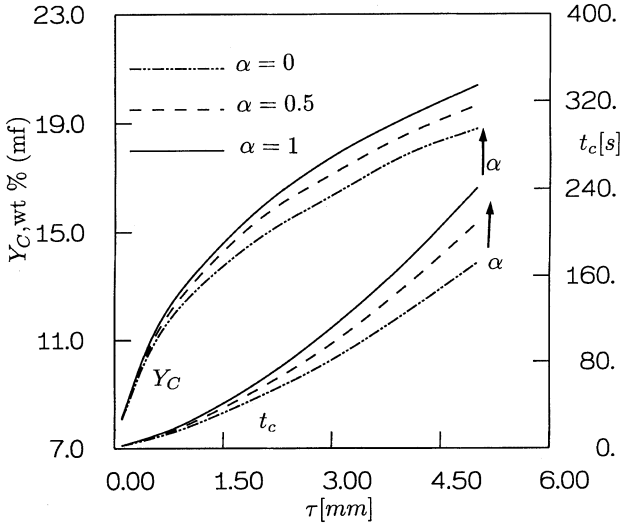

Figure 6. Char yields and conversion times as functions of the half-thickness of the particle as predicted for different particle shrinkage factors and $T_r = 800$ K (single-particle model).

shorter as the shrinkage factor is increased or a spherical geometry is considered.

Shrinkage alters the heat-transfer conditions across the particles, reducing internal resistances and thus favoring the attainment of higher reaction temperatures. This effect causes a predominance of the primary reaction path leading to liquid formation essentially at the expense of char and reduces the conversion times. In quantitative terms, maximum reductions in the particle size ($\alpha = 0$ against $\alpha = 1$) correspond to final sizes that are about 45–51% the initial value ($\tau = 0.1$–5 mm). These changes result in conversion times and char yields that are 96–71% and 99–92%, respectively, of the values obtained for nonshrinking particles. Hence, as shown by Figure 6, shrinkage plays a successively more important role as the particle size is increased, especially in relation to conversion times. However, the effects are globally small for fast pyrolysis conditions (in particular, for $\tau = 0.5$–1 mm, conversion times may be, in the best case, reduced by a factor of 20%).

By increasing the shrinkage level, the simultaneous increase in the degradation rate (gas velocity) and decrease in the thickness of the char layer shorten the intraparticle residence time of volatiles, thus reducing the activity of secondary reactions. This effect is, however, again negligible for the moderate temperatures and small sizes examined here.

For the range of τ previously given, the conversion times and the char yields simulated for spherical particles are 80–55% and 92–90%, respectively, of those simulated for slabs (intermediate values are simulated for cylindrical particles). Again the effects due to particle shape are enhanced as the sizes become larger and are quantitatively more important than shrinkage. In practical systems, however, a semi-infinite slab of defined thickness is a better approximation than a sphere for wood chips (Simmons and Gentry, 1986).

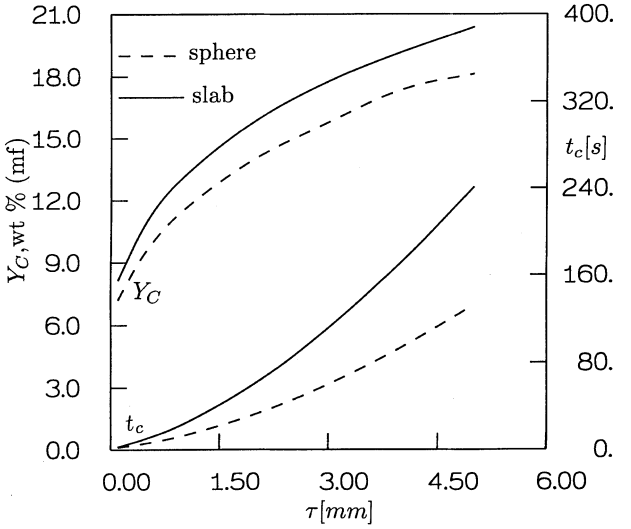

Figure 7. Char yields and conversion times as functions of the half-thickness of the particle as predicted for slab- and sphere-shaped particles and $T_r = 800$ K (single-particle model).

Influences of the external heat-transfer model

The actual external heat-transfer rates experienced by the wood particle in different units or in the same unit, as the conversion level varies, may be different, owing to the specific devices used to supply heat, the flow conditions, the mixing degree, the particle properties (highly variable in the course of the reaction process), and so on. Idealized conditions correspond to an infinitely fast external heat-transfer rate [the particle surface is equal to the external (reactor) temperature from the beginning of the degradation process, $T_s = T_r$, case a]. For good solid mixing, external heat-transfer coefficients are very high, as predicted by the Agarwal model used in the description of fluid-bed pyrolysis of wood proposed here (case b). However, this is somewhat problematic for biomass materials (Rasul and Rudolph, 2000), and segregation may cause particle conversion to take place above the sand bed. Thus, external heating rates can be more adequately described by the Ranz–Marshall correlation, which is representative of the convective heating of a single particle (Kunii and Levenspiel, 1991) (case c), or by a whole-bed coefficient, corresponding to a bed of particles heated by a hot gas stream (Kunii and Levenspiel, 1991) (case d). In order to evaluate the influences of the external heat-transfer model on the predictions of the pyrolysis process, simulations are compared with cases (a), (b), (c) and (d). Simulations are again made for τ between 0.1 and 5 mm and $T_r = 800$ K. The predictions of case (b) are used as a reference for comparison with the other cases.

The char yields and the conversion times are reported as functions of the particle half-thickness in Figure 8. As expected, qualitative trends are the same in all cases. Predictions of case (a) (infinitely fast external heat-transfer rates) are very close to those obtained for the reference case (b).

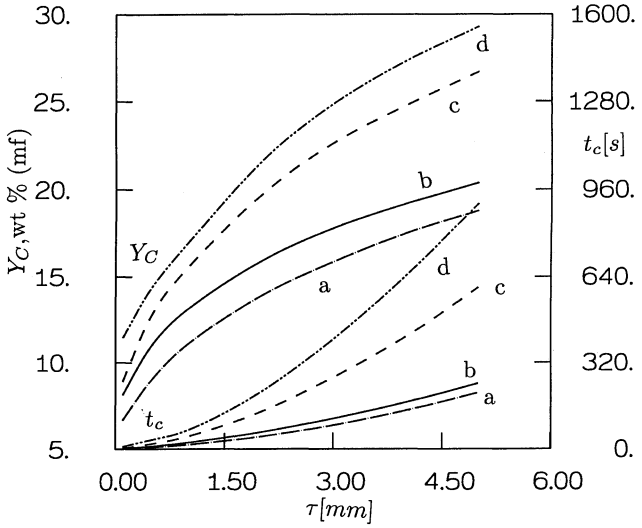

Figure 8. Char yields and conversion times as functions of the half-thickness of the particle as predicted for $T_r = 800$ K (single-particle model) and different external heat transfer (h) models.

(a) infinitely fast external heat transfer rate ($T_s = T_r$); (b) model by Agarwal (1991); (c) Ranz–Marshall correlation (Kunii and Levenspiel, 1991); (d) whole-bed correlation (Kunii and Levenspiel, 1991).

Indeed, the conversion times and char yields are 72–86% and 80–90%, respectively, of those of case (b). Differences tend to disappear as internal heat transfer becomes the controlling mechanism.

Predictions of the external heat-transfer coefficient for models (b), (c), and (d) are widely different. For $T_r = 800$ K and τ between 0.1 and 5 mm, against the values of 1,880–480 W/m^{2}K of the Agarwal model, the Ranz–Marshall and the whole-bed correlations, based on the superficial velocity, give ranges of 650–22 W/m^2 and 1.4–4.4 W/m^{2}K, respectively. Furthermore, while models (a) and (b) predict coefficients highly dependent on the particle size, with differences becoming successively higher, the whole-bed approximation presents values that aren't affected very much by the particle size.

The Ranz–Marshall correlation provides conversion times that are from 1.4 to 2.5 longer and char yields that are from 1.1 to 1.3 higher than those of model (b) as τ is increased. This is a result of the increased difference between the two heat-transfer coefficients with the particle size. Differences are very large between models (b) and (d), with conversion times longer by a factor of about 3.8 and char yields from 1.3 to 1.5 higher over the entire range of particle sizes examined.

Assuming that sizes corresponding to $\tau = 0.5$–1 mm represent fast pyrolysis conditions, in the ideal case, where the surface temperature becomes instantaneously equal to the reactor temperature, conversion takes about 6–15 s, with yields of char of 9–11%. These figures for the Agarwal model, which is a realistic approximation of the actual external heat-transfer rate between a particle and a fluid bed under conditions of good mixing, are 10–22s and 11–13%. Departures from these optimal operating conditions may result in conversion times of 18–42 s and char yields of 13–16% (Ranz–Marshall correlation), or even of 34–62 s and char yields of 15–17%. Hence, variations in the fluidization conditions can noticeably affect the fast pyrolysis characteristics.

Extraparticle Processes and Comparison Between Predictions and Experiments

In order to assess the validity of the model predictions from the quantitative point of view, the experimental results reported by Scott and Piskorz (1982, 1984), Scott et al. (1988), and Wehlte et al. (1997) are considered for comparison. These were preferred to other literature data [e.g., Horne and Williams (1996), and Peacocke et al. (1997)], because they were obtained for hardwoods, the same category used here for the determination of primary degradation kinetics, and were provided with sufficient information about the experimental conditions. The experiments were made through systems based on the same design [a shallow fluid bed, WFPP (Scott et al., 1999)] at a bench scale (15–50 g/h) (Scott and Piskorz, 1982; Wehlte et al., 1997) and pilot scale (2–3 kg/h) (Scott and Piskorz, 1984; Scott et al., 1988). Material used comprises poplar (Scott and Piskorz, 1982), poplar and maple (Scott and Piskorz, 1984; Scott et al., 1988) and beech (Wehlte et al., 1997). The apparent residence times of volatiles, t_v, were 0.44 s with reactor temperatures of 673-923 K and particle sizes of 0.25 mm (Scott and Piskorz, 1982) and 0.6 mm (Scott and Piskorz, 1984; Scott et al., 1988), and 1 s with reactor temperatures of 648–873 K and particle sizes of 0.3–0.5 mm (Wehlte et al., 1997). Furthermore, in Scott et al. (1988) results are also reported for high temperatures (923–1,050 K) and thin particles (0.1 mm) obtained by means of an entrained-bed reactor with $t_v = 0.44$.

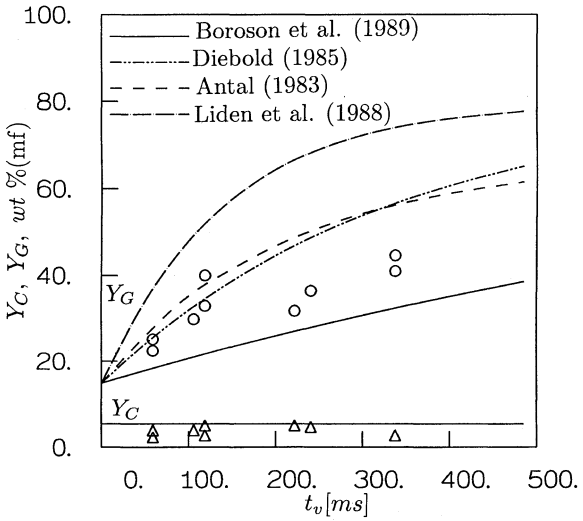

Figure 9. Gas and char yields (lines) as functions of the (extra-particle) residence time of volatiles as predicted for $\tau = 0.1$ mm and $T_r = 973$ K.

Craking of wood tar by Diebold (1985), Liden et al. (1988), and Boroson et al. (1989); cracking and polymerization of cellulose tar by Antal (1983). Experimental data (symbols) from Scott et al. (1988) (maple wood, entrained-bed reactor) are also included for comparison.

In order to keep it simple, the single-particle model assumes nonshrinking, slab-shaped particles and properties/kinetics of beech wood (as already used for the simulations presented earlier). For the extraparticle model, it is assumed that the aqueous fraction of the total liquids produced is constant and equal to 15%, wt. (moisture free) [contribution estimated according to the water content in bio-oil (Bridgwater, 1999), although it may increase slightly with the reaction temperature (Aguado et al., 2000)]. As anticipated, the residence time of tar vapors in a hot environment (T_r) is assumed to coincide with t_v or t_b. Also, tar degradation kinetics proposed by different authors are compared.

In the first place, the effects of the residence times of volatile products on the yields of liquids and gas have been simulated by varying t_v as in Scott et al. (1988), assuming an external heat-transfer coefficient of 1,800 W/m^2, $T_r = 973$ K and $\tau = 0.05$ mm (entrained-bed reactor). Figures 9 and 10 report the measured and predicted final product yields as functions of the residence time of volatiles. Given the very thin particles, intraparticle reactions of tar degradation do not occur, leading for zero extraparticle residence time of volatiles, to maximum liquid yields of 80%. The predicted char yields are about 7.5% and are in good agreement with measurements. Reaction kinetics of the cracking of wood tars, reported by Diebold (1985), Liden et al. (1988), Boroson et al. (1989), and cracking and polymerization of cellulose tars, reported by Antal (1983), are considered for extraparticle processes. The experiments indicate that, for residence times of about 500 ms, continuous conversion of the liquid compo-

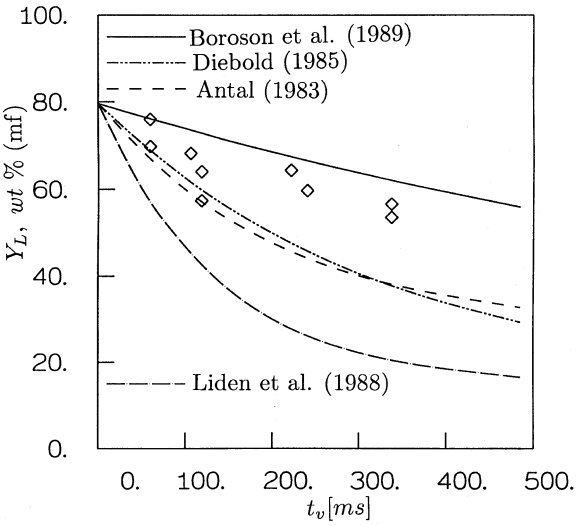

Figure 10. Liquid yields (lines) as functions of the (extra-particle) residence time of volatiles as predicted for $\tau = 0.1$ mm and $T_r = 973$ K.

Craking of wood tar by Diebold (1985), Liden et al. (1988), and Boroson et al. (1989); cracking and polymerization of cellulose tar by Antal (1983). Experimental data (symbols) from Scott et al. (1988) (maple wood, entrained-bed reactor) are also included for comparison purposes.

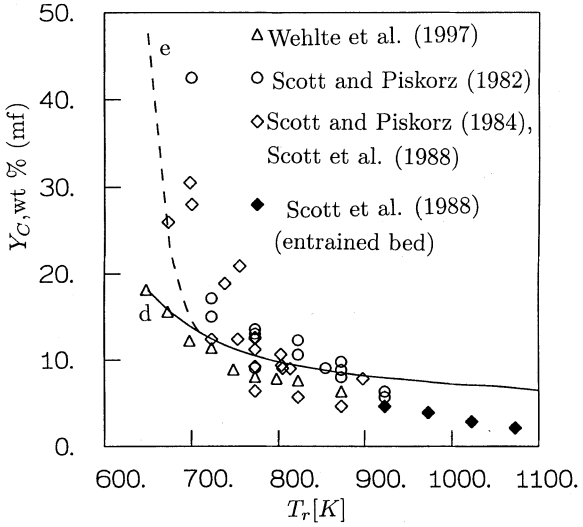

Figure 11. Char yields (lines) as functions of the reactor temperature as predicted for (d) $t_v = 0$, and (e) $t_s = 60$ s (intra- and extra-particle processes).

Experimental data (symbols) are also included for comparison.

nents to gases takes place until the two product classes attain a constant value (about 35%).

For short volatiles residence times, such as those of interest in fast pyrolysis, the kinetics of the cracking of wood tars to permanent gases examined here predict the conversion process qualitatively well. From the quantitative point of view, those by Diebold (1985) are barely acceptable, and in the other two cases the agreement is very poor. In particular, the kinetics by Liden et al. (1988) are the fastest and those by Boroson et al. (1989) the slowest. Moreover, contrary to experimental evidence that indicates that catalysts and/or adequate thermal conditions are necessary for the destruction of tars as, for instance, in the cleaning of the producer gas (Maniatis, 2001), in all cases, sufficiently long complete conversion of the organic fractions occurs for residence times.

For residence times below 500 ms, the mechanism of competitive reactions a4–a5, associated with the kinetic constants given by Antal (1983), predict gas and liquid (water plus refractory tar) yields very close to those of the Diebold kinetics. In addition, an ultimate yield of refractory tar of about 13% is obtained which, from the qualitative point of view, leads to better agreement with experimental observation.

The highly simplified treatment of the transport phenomena for the entrained-bed reactor does not allow conclusive remarks to be made about the effectiveness of the kinetics currently available for secondary degradation of tars. However, the results of Figures 9 and 10 show that they predict the correct order of magnitude of the reaction rate. In addition, quantitative predictions presumably can be obtained only through the use of the reaction mechanism a4–a5, which takes the different reactivity of at least two different fractions of tar vapors into account. Further experimental analysis is, however, required in order to evaluate the kinetic constants for wood tars.

Figures 11–13 allow a comparison to be made between measured and predicted product yields as functions of the reactor temperature. Simulations have been made with $\tau =$ 0.3 mm and external temperatures between 650 and 1,100 K. Solid lines (d) represent the predicted product distribution in the absence of extraparticle vapor cracking and solid residence times coincident with the conversion times. The dashed

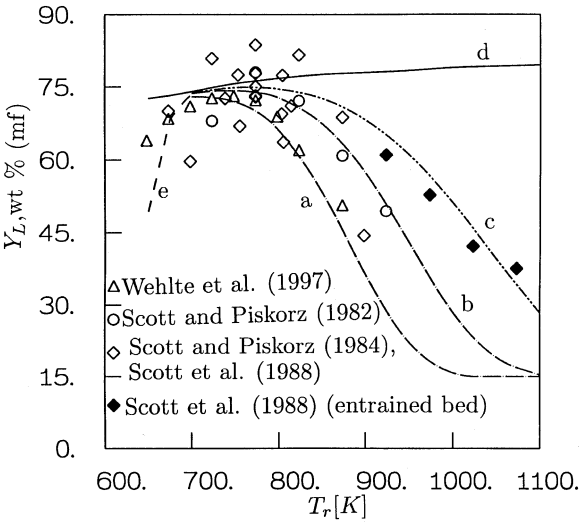

Figure 12. Liquid yields (lines) as functions of the reactor temperature as predicted for $\tau = 3$ mm.

(a) $t_v = 0.44$ s [tar cracking kinetics by Liden et al. (1988)]; (b) $t_b = 0.154$ s [tar cracking kinetics by Liden et al. (1988)]; (c) $t_v = 0.44$ s [tar cracking kinetics by Boroson et al. (1989)]; (d) $t_v = 0$; and (e) $t_s = 60$ s. Experimental data (symbols) are also included for comparison.

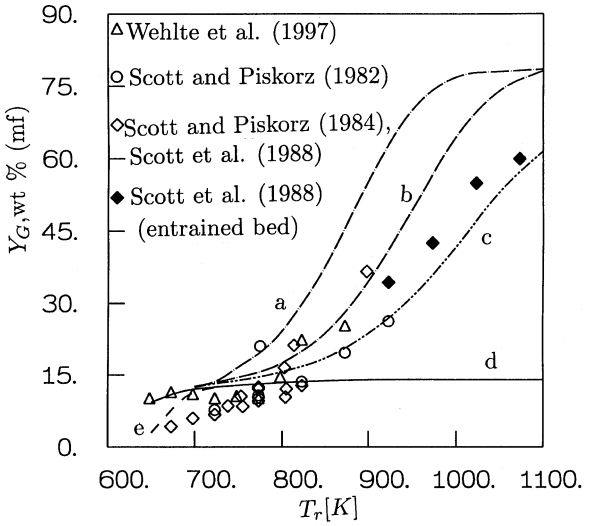

Figure 13. Gas yields (lines) as functions of the reactor temperature as predicted for $\tau = 0.3$ mm.

(a) $t_v = 0.44$ s [tar cracking kinetics by Liden et al. (1988)]; (b) ($t_b = 0.154$ s [tar cracking kinetics by Liden et al. (1988)]; (c) $t_v = 0.44$ s [tar cracking kinetics by Boroson et al. (1989)]; (d) $t_v = 0$; and (e) $t_s = 60$ s. Experimental data (symbols) are also included for comparison purposes.

lines (e) (Figures 11–13), which are shown for temperatures below 700 K, are representative of conversion conditions attained for a 60-s residence time of the wood particles. The three dashed-dotted lines (a, b, c) ($T_r \geq 700$ K, Figures 12 and 13) report the simulation results obtained in the presence of extraparticle processes. The curves have been obtained for $t_b = 0.154$s (curves b) and for $t_v = 0.44$s (curves a) according to the kinetics by Liden et al. (1988). For this t_v value, the volatile product distribution also has been simulated according to the kinetics by Boroson et al. (1989) (curves c).

Char (Figure 11) is a product of primary reactions only. When complete conversion is considered (curve d), the agreement between predictions and measurements reported by Wehlte et al. (1997) is good over the entire range of temperatures examined. The agreement with the fluid-bed data by Scott and coworkers is good for high (above 700 K) temperatures, when particle conversion occurs within times of 42 s ($T_r = 700$ K) and 2.5 s ($T_r = 923$ K). For the entrained-bed data, the higher char yields predicted by the model are due to the thicker particles used in the simulations (0.6 mm against 0.1 mm, see also Figure 9). At low temperatures (< 700 K), large scatter is observed in the experimental measurements, but these are clearly higher than the simulations obtained for complete conversion, which, for the lowest temperature, takes about 266 s.

A rapid increase in the total solid yields is simulated when particles are allowed to remain in the high-temperature reaction environment for a maximum time of 60 s (curve e). Indeed, the solid residence time, which can be significantly affected by the size of the conversion unit, is an important parameter for the conversion level, especially when external temperatures are barely sufficient for the degradation process to occur.

In fluid-bed reactors, independent of secondary-reaction activity, gas velocities should be high to obtain good solid (sand and biomass) mixing, but wood particles can be elutriated before complete conversion is attained. For conditions used in fast pyrolysis, solid residence times have been reported to be 1–5 s (Scott and Piskorz, 1984) or, for bench-scale units, 120–180 s (Scott and Piskorz, 1982). Consequently, for reactor temperatures below 700 K, the solid residence time may be not long enough for conversion to be completed and the measured yields of charred solid may also contain unpyrolyzed wood. In particular, for reactor temperatures below 725 K, the yields of char from beech wood particles pyrolyzed in a sweeping gas stream (Beaumont and Schwob, 1984) are lower than those reported by Scott and coworkers. It can be assumed that, despite the slower external heat-transfer rates of convective heating compared with those of sand-fluidized reactors, wood particles reside in the hot reactor environment until complete conversion. For the data reported by Wehlte et al. (1997), it is also likely that, given the lower velocities of the bench-scale unit, no significant particle elutriation occurs before conversion.

As discussed earlier, the actual external heating rate experienced by the particle can be significantly affected by the mixing conditions. Deterioration of mixing appears as an increase in the yields of char (and longer conversion times). Although there is no evidence for mixing problems at low temperatures, it is interesting to note that these could provide a plausible explanation for the high char yields (above 20%) in some cases reported for small-sized particles and fluid-bed conversion (Horne and Williams, 1995; Peacocke et al., 1997; not shown in figure). Indeed, they are comparable with those measured for thick (20–50 mm) wood (Belleville and Capart, 1984; Chan et al., 1985; Gronli, 1996; Di Blasi et al., 2001a,b).

Good quantitative agreement is observed between predictions and measurements in terms of maximum liquid yields (Figure 12), which is observed for temperatures between 725 and 800 K. For lower temperatures, predictions are slightly higher for complete conversion (curve d) and slightly lower for solid residence times of 60 s (curve e). Gas yields (Figure 13) tend to be higher than measurements [good agreement is obtained only for complete conversion and the data by Wehlte et al. (1997)]. There could be a couple of explanations for these results, the first related to the wood variety, the second to kinetic modeling. Kinetic constants for the formation of the different product classes were estimated for beech wood, whereas the experimental data by Scott and coworkers (1982, 1984, 1988) were obtained for other hardwood varieties. A comparison between different varieties has shown (Di Blasi et al., 2001a) that beech wood produced the largest amount of gas [differences up to 5%, wt. (moisture free)]. Moreover, when reactor temperatures are low (below 700 K) and solid residence times shorter than conversion times, the details of the degradation process, associated with the behavior of the main wood constituents, may become important. Indeed, it can be postulated that, at low temperature, mainly holocellulose pyrolysis occurs, leading to liquid formation, whereas lignin, being less reactive, does not undergo significant reaction (with gas production). These features are not, however, accounted for by the one-stage mechanism used in this study.

For temperatures above 800 K, the dependence of the yields of volatile products on temperature is determined by extraparticle degradation of tars. The decay in the yields of liquids and the corresponding increase in the yields of gas, as the fluid-bed temperature is increased, is described with acceptable accuracy (within the range of the scatter of measurements) by the Liden kinetics coupled with the limit values of the residence time of volatiles previously introduced (t_v, t_b). It is also worth noting that these kinetics also gave acceptable predictions for the yields of products from the fluid-bed pyrolysis of cellulose (Di Blasi, 2000b). In accordance with the analysis reported for Figures 9 and 10, on the other hand, better predictive capabilities are shown by the Boroson kinetics for the entrained-bed reactor (high-temperature data and t_v).

Conclusions

A detailed mathematical model for single-particle processes has been coupled with a simplified description of extraparticle processes to predict the characteristics of the fast pyrolysis of wood in fluid-bed reactors, a topic not addressed in previous literature. For conditions of interest in fast pyrolysis (particle sizes of 0.1–6 mm and a reactor temperature of 800 K), actual heating rates experienced by wood particles are roughly between 450 and 5 K/s and actual reaction temperatures are between 770 and 640 K. Convective transport of the volatile products of pyrolysis is the main factor responsible for particle dynamics. The effects of particle shrinkage and shape are scarcely important for small-sized particles and mainly appear as variations in the conversion times. Variations in the external heat-transfer rates, caused by poor solid mixing and/or segregation, are quantitatively more important and affect both conversion times and product yields.

The model predicts with acceptable accuracy the product yields for reactor temperatures in the 650–950 K range. For reactor temperatures below 800 K and apparent residence times of volatiles typically achieved in fast pyrolysis devices (0.5 s), product yields are determined by single-particle behavior. Hence, given the small sizes (below 6 mm), intraparticle degradation of tars is again negligible. The conversion time that should be at least equal to the residence time of particles within the hot-reactor environment is a critical parameter. Indeed, before all the pyrolysis products are swept from the reactors to cyclones, where a large part of char is separated from gas and vapors, it is highly desirable to attain the highest conversion of wood to volatiles. It is understood that this may be problematic at very low temperatures (below 700 K), which, however, are not of interest in practical applications. Systematic measurements of the devolatilization times of single wood particles in fluid-bed reactors, currently not available, could be useful for improving the operating conditions of industrial reactors and the validation of currently available transport models.

For reactor temperatures above 800 K and the small-sized particles of fast pyrolysis technologies, the product yields are essentially determined by the extraparticle activity of tar degradation reactions even for the short residence times of fast pyrolysis units. Estimations of chemical kinetics derived from the literature correctly predict the magnitude of the reaction rates to be used for optimization and scaling purposes. To improve the predictive capabilities of the models, further research is needed to understand the role played by the chemistry of tars in the subsequent degradation process.

Acknowledgment

The research was funded in part by the European Commission.

Thanks are also due to the anonymous reviewers for their useful comments on the manuscript.

Notation

A = preexponential factor, s^{-1}
B = intrinsic permeability, m^2
c = heat capacity, kJ/kg·K
D_0 = diffusion coefficient, m^2/s
d = particle pore diameter, m
D_r = reactor diameter, m
d_s = sand-particle diameter, μm
e = surface emissivity
E = activation energy, kJ/mol
H = expanded bed height, m
h = global heat-transfer coefficient, $kW/m^2 \cdot K$
L = reactor height, m
k = Arrhenius constant, s^{-1}
T = temperature, K
T_c = temperature at the particle center, K
T_r = reactor temperature, K
T_s = temperature at the particle surface, K
t = time, s
t_c = conversion time, s
t_b = volatile residence time (H/U_b), s
t_v = volatile residence time (V/F), s
t_s = solid residence time, s
U_b = bubble velocity (reactor), m/s
U_{mf} = minimum fluidization velocity (reactor), m/s
u = intraparticle gas velocity, m/s
x = space, m
Y = mass fraction
Y_C, Y_G, Y_L = char, gas, and liquid yields, % by weight (wt.) of dry (mf) wood

Greek letters

α = shrinkage factor
β = heating rate, K/s
ϱ = density, kg/m^3
ϵ = particle porosity
λ = thermal conductivity, W/m·K
μ = viscosity, kg/ms
ω = pore emissivity
τ = particle half-thickness, mm

Subscripts

C = char
G = gas
g = total volatiles (tar + gas)
L = liquid
s = secondary
S = wood
0 = initial or reference conditions

Literature Cited

Agarwal, P. K., "Transport Phenomena in Multi-Particle Systems—IV. Heat Transfer to a Large Freely Moving Particle in Gas Fluidized Bed of Smaller Particles," *Chem. Eng. Sci.*, **46**, 1115 (1991).

Aguado, R., M. Olazar, M. J. San Jose, G. Aguirre, and J. Bilbao, "Pyrolysis of Sawdust in a Conical Spouted Bed Reactor. Yields and Product Composition," *Ind. Eng. Chem. Res.*, **39**, 1925 (2000).

Antal, M. J., "Biomass Pyrolysis: A Review of the Literature: I. Carbohydrate Pyrolysis," *Advances in Solar Energy*, K. W. Boer and J.

A. Duffie, eds. American Solar Energy, Boulder, CO, p. 61 (1982).
Antal, M. J., "Effects of Reactor Severity on the Gas-Phase Pyrolysis of Cellulose- and Kraft Lignin-Derived Volatile Matter," *Ind. Eng. Prod. Res. Dev.*, **22**, 366 (1983).
Antal, M. J., "Biomass Pyrolysis: A Review of the Literature: II. Lignocellulose Pyrolysis," *Advances in Solar Energy*, Vol. 2, K. W. Boer and J. A. Duffie, eds.; Plenum Press, New York, p. 175 (1985a).
Antal, M. J., "A Review of the Vapor Phase Pyrolysis of Biomass Derived Volatile Matter," *Fundamentals of Thermochemical Biomass Conversion*, R. P. Overend, T. A. Milne, L. K. Mudge, eds., Elsevier Applied Science, New York, p. 511 (1985b).
Antal, M. J., and G. Varhegyi, "Cellulose Pyrolysis Kinetics: The Current State of Knowledge," *Ind. Eng. Chem. Res.*, **34**, 703 (1995).
Antal, M. J., E. Croiset, X. Dai, C. De Almeida, W. S. L. Mok, N. Norberg, J. R. Richard, and M. A. Majthoub, "High-Yield Biomass Charcoal," *Energy Fuels*, **10**, 652 (1996).
Antal M. J., S. G. Allen, X. Dai, B. Shimizu, M. S. Tom, and M. G. Gronli, "Attainment of the Theoretical Yield of Carbon from Biomass," *Ind. Eng. Chem. Res.*, **39**, 4024 (2001).
Beaumont, O., and Y. Schwob, "Influence of Physical and Chemical Parameters on Wood Pyrolysis," *Ind. Eng. Chem. Proc. Des. Dev.*, **23**, 637 (1984).
Belleville P., and R. Capart, "Pyrolysis of Large Wood Samples," *Appl. Energy*, **16**, 223 (1984).
Boroson, M. L., J. B. Howard, J. P. Longwell, and A. W. Peters, "Products Yields and Kinetics from the Vapor Phase Cracking of Wood Pyrolysis Tars," *AIChE J.*, **35**, 120 (1989).
Bridgwater, A. V., "Principles and Practice of Biomass Fast Pyrolysis Processes for Liquids," *J. Anal. Appl. Pyrolysis*, **51**, 3 (1999).
Chan, W. R., M. Kelbon, and B. B. Krieger, "Modelling and Experimental Verification of Physical and Chemical Processes During Pyrolysis of Large Biomass Particle," *Fuel*, **64**, 1505 (1985).
Diebold, J. P., "The Cracking Kinetics of Depolymerized Biomass in a Continuous Tubular Reactor," PhD Thesis, Colorado School of Mines, Golden (1985).
Di Blasi, C., "Modeling and Simulation of Combustion Processes of Charring and Non-charring Solid Fuels," *Prog. Energy Combust. Sci.*, **19**, 71 (1993).
Di Blasi, C., "Kinetic and Heat Transfer Control in the Slow and Flash Pyrolysis of Solids," *Ind. Eng. Chem. Res.*, **35**, 37 (1996a).
Di Blasi, C., "Heat Transfer Mechanisms and Multi-Step Kinetics in the Ablative Pyrolysis of Cellulose," *Chem. Eng. Sci.*, **51**, 2211 (1996b).
Di Blasi, C., "Heat, Momentum and Mass Transfer Through a Shrinking Biomass Particle Exposed to Thermal Radiation," *Chem. Eng. Sci.*, **51**, 1121 (1996c).
Di Blasi, C., "Comparison of Semi-Global Mechanisms for Primary Pyrolysis of Lignocellulosic Fuels," *J. Anal. Appl. Pyrolysis*, **47**, 43 (1998a).
Di Blasi, C., "Physico-Chemical Processes Occurring Inside a Degrading Two-Dimensional Anisotropic Porous Medium," *Int. J. of Heat Mass Transfer*, **41**, 4139 (1998b).
Di Blasi, C., "The State of the Art of Transport Models for Charring Solid Degradation," *Polym. Int.*, **49**, 1133 (2000a).
Di Blasi, C., "Modelling the Fast Pyrolysis of Cellulosic Particles in Fluid-Bed Reactors," *Chem. Eng. Sci.*, **55**, 5999 (2000b).
Di Blasi, C., E. Gonzalez Hernandez, and A. Santoro, "Radiative Pyrolysis of Single Moist Wood Particles," *Ind. Eng. Chem. Res.*, **39**, 873 (2000).
Di Blasi, C., C. Branca, A. Santoro, and R. A. Perez Bermudez, "Weight Loss Dynamics of Wood Chips Under Fast Radiative Heating," *J. Anal. Appl. Pyrolysis*, **57**, 77 (2001a).
Di Blasi, C., C. Branca, A. Santoro, and E. Gonzalez Hernandez, "Pyrolytic Behaviour and Products of Some Wood Varieties," *Combust. Flame*, **124**, 165 (2001b).
Di Blasi, C., and C. Branca, "Kinetics of Primary Product Formation from Wood Pyrolysis," *Ind. Eng. Chem. Res.*, **40**, 5547 (2001).
Gronli, M. G., "A Theoretical and Experimental Study of the Thermal Degradation of Biomass," PhD Thesis, NTNU, Trondheim, Norway (1996).
Horne, P. A., and P. T. Williams, "Influence of Temperature on the Products from the Flash Pyrolysis of Biomass," *Fuel*, **75**, 1051 (1996).
Janse, A. M. C., "A Heat Integrated Rotating Cone Reactor System for Flash Pyrolysis of Biomass," PhD Thesis, The Univ. of Twente, Twente, The Netherlands (1998).
Kothari, V., and M. J. Antal, "Numerical Studies of the Flash Pyrolysis of Cellulose," *Fuel*, **64**, 1487 (1985).
Kunii, D., and O. Levenspiel, *Fluidization Engineering*, Butterworth-Heinemann, Stoneham, MA (1991).
Lanzetta M., C. Di Blasi, and F. Buonanno, "An Experimental Investigation of Heat Transfer Limitations in the Flash Pyrolysis of Cellulose," *Ind. Eng. Chem. Res.*, **36**, 542 (1997).
Liden, A. G., F. Berruti, and D. S. Scott, "A Kinetic Model for the Production of Liquids from the Flash Pyrolysis of Biomass," *Chem. Eng. Commun.*, **65**, 207 (1988).
Maniatias, K., "Progress in Biomass Gasification: An Overview," *Progress in Biomass Thermochemical Conversion*, Vol. 1, A. V. Bridgwater, ed., Blackwell, Oxford, p. 1 (2001).
Narayan, R., and M. J. Antal, "Thermal Lag, Fusion, and the Compensation Effect During Biomass Pyrolysis," *Ind. Eng. Chem. Res.*, **35**, 1711 (1996).
Peacocke, C. G. V., C. M. Dick, R. A. Hague, L. A. Cooke, and A. V. Bridgwater, "Comparison of Ablative and Fluid Bed Fast Pyrolysis: Yields and Analyses," *Developments in Thermochemical Biomass Conversion*, A. V. Bridgwater and D. G. B. Boocock, eds., Blackie, London, p. 191 (1997).
Rasul, M. G., and V. Rudolph, "Fluidized Bed Combustion of Australian Bagasse," *Fuel*, **79**, 123 (2000).
Scott, D. S., and J. Piskorz, "The Flash Pyrolysis of Aspen-Poplar Wood," *Can. J. Chem. Eng.*, **60**, 666 (1982).
Scott, D. S., and J. Piskorz, "The Continuous Flash Pyrolysis of Biomass," *Can. J. Chem. Eng.*, **62**, 404 (1984).
Scott, D. S., J. Piskorz, M. A. Bergougnou, R. Graham, and R. P. Overend, "The Role of Temperature in the Fast Pyrolysis of Cellulose and Wood," *Ind. Eng. Chem. Res.*, **27**, 8 (1988).
Scott, D. S., P. Majerski, J. Piskorz, and D. Radlein, "A Second Look at Fast Pyrolysis of Biomass—The RTI Process," *J. Anal. Appl. Pyrolysis*, **51**, 23 (1999).
Shafizadeh, F., and P. P. S. Chin, "Thermal Deterioration of Wood," *ACS Symp. Ser.*, **43**, 57 (1977).
Shafizadeh, F., R. H. Furneaux, T. G. Cochran, J. P. Scholl, and Y. Sakai, "Production of Levoglucosan and Glucose from Pyrolysis of Cellulosic Materials," *J. Appl. Polym. Sci.*, **23**, 3525 (1979).
Simmons, G. M., and M. Gentry, "Particle Size Limitations Due to Heat Transfer in Determining Pyrolysis Kinetics of Biomass," *J. Anal. Appl. Pyrolysis*, **10**, 117 (1986).
Stewart, W. E., "Comments on 'Effect of Vapor Efflux from a Spherical Particle on Heat Transfer from a Hot Gas'," *Ind. Eng. Chem. Fundam.*, **23**, 268 (1984).
Stubington, J. F., and D. Sasongko, "On the Heating Rate and Volatile Yield for Coal Particles Injected into Fluidised Bed Combustors," *Fuel*, **77**, 1021 (1998).
Wagenaar, B. M., W. Prins, and W. P. M. van Swaaij, "Flash Pyrolysis Kinetics of Pine Wood," *Fuel Process Technol.*, **36**, 291 (1994).
Wagenaar, B. M., "The Rotating Core Reactor for Rapid Thermal Solids Processing," PhD Thesis, The Univ. of Twente, Twente, The Netherlands (1994).
Wehlte, S., D. Meier, J. Moltran, and O. Faix, "The Impact of Wood Preservatives on the Flash Pyrolysis of Biomass," *Developments in Thermochemical Biomass Conversion*, A. V. Bridgwater and D. G. B. Boocock, eds., Blackie, London, p. 206 (1997).

Manuscript received July 27, 2001, and revision received Feb. 4, 2002.